Earth Reinforcement Practice, Ochiai, Hayashi & Otani (eds) © 1992 Balkema, Rotterdam. ISBN 90 5410 093 1

Measurement and interpretation of reinforcement stresses in the APSR cell

A.J.Whittle, J.T.Germaine, D.G.Larson & M.Abramento
Massachusetts Institute of Technology, USA

ABSTRACT: Laboratory measurements in direct shear box and pullout tests are routinely used to characterize parameters of soil-reinforcement interaction such as direct sliding resistance and bond capacity, for limit equilibrium design calculations. More comprehensive studies of soil-reinforcement interaction are necessary in order to predict the stress distribution in the reinforcements at working load levels. The mechanisms of interaction are particularly complex for inclusions with non-planar geometries, such as grids, and for materials such as geosynthetics which exhibit non-linear and time dependent behavior.

This paper describes a new laboratory device, referred to as the Automated Plane Strain Reinforcement (APSR) cell, for measuring the stresses which develop within a reinforcing inclusion due to shearing of the surrounding soil. The APSR cell has the capability of measuring directly the maximum tensile stress at the center of the inclusion as well as the local stress and/or strain distribution within reinforcements of various lengths and geometries. Typical data are presented for an instrumented steel sheet inclusion embedded in Ticino sand. An approximate 'shear lag' analysis has been developed in order to predict the load transfer in the APSR cell, based on known properties of the soil and reinforcing material. Direct comparisons show excellent agreement with the APSR data for the elastic steel sheet inclusion.

1. INTRODUCTION

Geosynthetic materials are widely used to reinforce soil masses in the construction of retaining walls, embankments, foundations and pavements. The performance of these composite soil structures depends, in large part, on the interaction between the soil matrix and the inclusions which determines the magnitude of loads carried by the reinforcements. There are two main approaches currently used in studies of soil-reinforcement interaction: 1) equivalent homogenization methods, which treat the reinforced soil (macroscopically) as an homogeneous, anisotropic composite material; and 2) limit equilibrium methods of stability analysis, which evaluate simplified modes of interaction.

Homogenization methods typically assume that the soil mass is reinforced with uniform, closely spaced inclusions such that explicit modelling of load transfer between the soil and reinforcement is not considered. Failure of composite reinforced soils has been investigated experimentally using small scale triaxial or direct shear tests. For example, Schlosser and Long (1972) present results which show that the reinforcements produce an apparent cohesive strength component that is directly proportional to the density and strength of the reinforcing inclusions (aluminium foil disks). However, scale effects associated with these tests are not readily evaluated and hence, the data cannot be extrapolated to prototype field situations.

Current design methods for reinforced soil masses are all based on limit equilibrium analyses (e.g. Jewell, 1990). These calculations postulate different mechanisms of failure and assume that stability of the structure is maintained either through: a) sliding resistance along the soil-reinforcement interface, or b) tensile stresses generated in the reinforcement and resisted by a bond (anchor) length embedded in the stable soil mass. There are two principal laboratory tests used to measure input parameters for these calculations: 1) direct shear box tests, which measure the interface friction; and 2) pull-out tests, which are used to estimate the bond resistance. These tests suffer from a number of well known practical limitations associated with poorly controlled boundary conditions, and are especially difficult to interpret for relatively extensible reinforcements, such as geosynthetics, and for inclusions with non-planar geometries, such as grids.

Further studies (e.g., Jewell and Wroth, 1987; Shewbridge and Sitar, 1989) have observed the deformations of reinforcements which intersect the horizontal failure plane, at various orientations, in direct shear box tests. These measurements enable indirect computation of maximum tensile stresses at failure, based on limit equilibrium calculations within the failure zone. However, the analyses are affected significantly by the width of the failure zone and cannot be extended reliably to predict reinforcement stresses in pre-failure conditions.

Overall, the above discussion shows that although existing laboratory tests provide design parameters for limit equilibrium analyses, they are not well suited for estimating load transfer characteristics, especially at working load levels. Primary limitations of existing tests are due to: a) non-uniformity of stress and strain conditions within the soil; b) lack of direct measurements of loads carried by the reinforcing materials. This paper summarizes the development of a new laboratory device, referred to as the APSR cell, which has the rather unique capability of measuring directly the development of maximum tensile stress and load distribution within a reinforcing inclusion, due to shearing of the surrounding soil. The device imposes plane strain boundary conditions which are representative of many practical field situations where earth reinforcement is used (e.g., embankments, retaining walls etc.). The interpretation of test measurements can be achieved using simplified analytical solutions developed by Abramento and Whittle (1992). The test data provide a basis for evaluating the performance of soil reinforcements at working load levels.

2. THE APSR CELL

Figures 1 and 2 show schematic diagrams of the Automated Plane Strain reinforcement (APSR) cell developed at MIT (Larson, 1992; Whittle et al., 1991). The cell is designed to measure the maximum tensile stress, which is transferred to a reinforcing inclusion as the surrounding soil deforms in plane strain shearing, due to the application of uniform boundary tractions ($\sigma_{yy}=\sigma_1$, $\sigma_{xx}=\sigma_3$; Fig. 1). Measurements of stress and/or strain distributions within the inclusion can also be obtained through additional instrumentation.

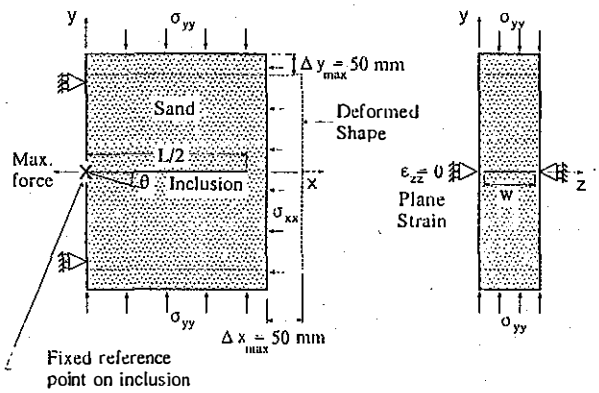

Fig. 1 Schematic diagram of the APSR cell

The APSR cell uses a soil specimen of overall dimensions 570mm high, by 450mm wide, by 150mm deep (plane strain direction), which is enclosed by a thin rubber membrane. The specimen can contain a single reinforcing inclusion up to 450mm in length (L/2; Fig. 1), which can be oriented at different angles to the direction of the applied principal stresses ($\theta=\pm 50^0$, Fig. 1).

The key design feature of the APSR design is that the inclusion is clamped externally to a load cell, such that the plane through which the inclusion enters the cell (i.e., x=0; Fig. 1) is also a plane of symmetry in the specimen. In order to maintain this symmetry, the position of the reinforcement is controlled by a hydraulic piston such that there is no displacement of the reinforcing inclusion at the entry point, marked X in Figure 1 (Larson, 1992). Thus, the point X represents the center of an inclusion of total length, L, and the load cell then measures the maximum tensile stress which occurs at this location. The APSR cell is conceptually similar to the 'unit cell' developed by McGown et al., (1978), but has the additional capability for measuring directly the tensile stresses in the reinforcement.

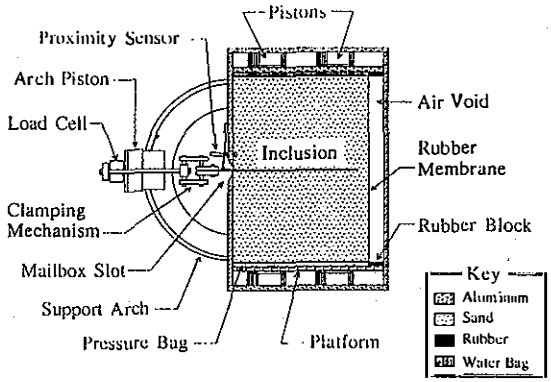

Fig. 2 Section through the APSR cell

Figure 2 shows that the reinforcement load cell reacts, through a hydraulically operated piston against a structural arch such that the position of the reference point can be maintained through feedback control. The inclusion enters the cell through a mailbox slot which can be specially designed for reinforcements up to 10mm deep. The following paragraphs summarize the principal design features of the APSR cell (Larson, 1992):

1. The length of the reinforcing inclusion is an important factor in selecting the dimensions for the APSR cell. For a given set of material properties (soil and reinforcement), the length of the reinforcement affects the maximum tensile stress that is transferred to the inclusion. Analyses show that prototype, field conditions can be simulated using inclusions with half-lengths, L/2= 1.0 to 2.0m (Whittle et al., 1991), which are beyond the scale that can be readily acheived in the laboratory. Instead, dimensions of the APSR cell are sufficient to handle commercially available geogrid materials (e.g., McGown et al., 1985), while measurements for different lengths of inclusion provide a basis for estimating field stresses.
2. The magnitudes of the applied boundary tractions determine the structural design of the APSR cell. The device can apply a major principal stress,

$\sigma_1 \leq 500$kPa (Fig. 1) through two pressurized water bags mounted on moveable rigid platforms. Uniform lateral confinement, $\sigma_3 \leq 50$kPa is provided by air pressure acting on the rubber membrane which encloses the soil specimen. All contact surfaces are lubricated with silicon grease in order to minimize friction in the system. Overall, the design ensures the uniformity of exterior stresses in the soil specimen.

3. The cell can impose axial strains of up to 10% on the specimen (approximately 100mm platen to platen movement) which are sufficient to cause failure of unreinforced sand specimens and to develop maximum loads transfer even for relatively extensible geosynthetic reinforcements (cf. Palmeira and Milligan, 1989). Plane strain conditions are achieved through an active system using a pressurized water diaphragm within the side walls. This novel design reduces significantly the size of the walls that would otherwise be required, and enables remote measurement of the strain field in the specimen using radiography. Maximum lateral strains in the sample are less than 0.01%.
4. The APSR cell is fully automated and includes eight independent feedback control systems for the pressures in the drive pistons, lateral diaphragm walls, arch support piston and confining air pressure. These are controlled by a single microcomputer and three custom-built, analog feedback circuits. Automation provides great flexibility in test procedures and enables soil specimens to be sheared under conditions of stress or displacement control. These capabilities are particularly useful in measuring load transfer for geosynthetic reinforcements which exhibit significant time dependent properties (e.g., Wilding and Ward, 1978). Instrumentation for the control of boundary tractions and displacements includes: a) a proximity sensor to monitor the reference position, **X** (Fig. 2); b) pressure transducers, which measure the hydraulic pressure in the water bags and the confining air pressure; c) displacement transducers, which monitor and control the movement of the platforms and side walls; and d) additional displacement transducers measure directly the axial and lateral deformation of the specimen.
5. Sand specimens are prepared by raining particles through an assembly of sieves. The raining apparatus can produce either loose or dense sand specimens with uniform density (Larson, 1992). However, the depositional process also introduces a structure or fabric such that the mechanical properties of the sand are cross-anisotropic (e.g., Arthur and Menzies, 1972). The APSR cell is designed such that the specimen can be deposited along either the z or y axes (Fig. 1). Sand samples deposited in the z direction initially exhibit isotropic properties for plane strain shearing in the x-y plane, while those formed in the y-direction have cross-anisotropic properties. This important design feature decouples the effects of soil anisotropy in the measurements of load transfer using the APSR cell.
6. The external load cell measures the maximum tensile force in the reinforcement at the reference location **X** (Fig. 1). Additional instrumentation can be designed to measure local strains and/or stresses at locations along the inclusion, for different types of reinforcing material. Deformations within the soil specimen are computed from radiographic measurements of the displacements of tungsten-steel markers embedded in the cell (Arthur, 1977).

Larson (1992) describes the extensive program of proof tests which have been performed in order to evaluate the design and performance of the APSR cell. All of these tests use dry Ticino sand as the reference soil. The physical and engineering properties of Ticino sand are typical of many natural sands and are well documented in the literature (e.g., Baldi et al., 1985). The sand is deposited along the z-axis of the APSR cell (Fig. 1) with initial relative densities, $D_r \approx 30$ and 75% (loose and dense specimens, respectively). The proof tests have: a) established that the silicon grease lubrication is successful in minimizing wall friction in the APSR cell; and b) refined test procedures such that measurements of stress-strain behaviour for the unreinforced sand are repeatable and consistent. The stress-strain-strength properties of the unreinforced Ticino sand, measured in the APSR cell, are in good agreement with results from other plane strain devices reported by Marachi et al. (1981).

3. STRESSES IN A STEEL SHEET INCLUSION

The first program of load transfer measurements in the APSR cell were obtained for elastic, two-ply steel sheet inclusions. In addition to the external load measurement, the tests include local measurements of

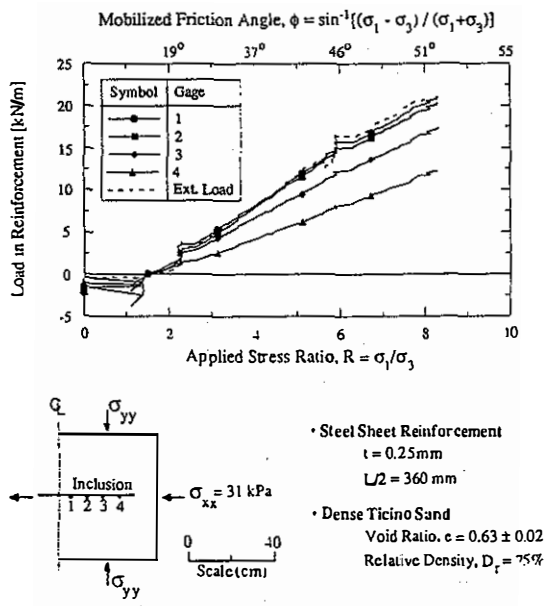

Fig. 3 Typical measurements of stresses in a steel sheet inclusion

the strain distribution within the reinforcement from a series of strain gauges sandwiched between the two thin steel sheets (each 0.13mm thick). In-isolation uniaxial tension tests are first performed on the inclusion in order a) to measure the modulus of the steel, and b) to check the performance and calibration of the strain gauges. Figure 3 shows typical measurements of the reinforcement stresses in an inclusion of half-length, L/2=0.36m, for shearing of dense Ticino sand at a confining pressure, σ_3=31kPa. The figure reports the reinforcement stresses, measured at the centerline and at four locations along the inclusion, as functions of the external stress ratio in the soil, $R=\sigma_1/\sigma_3$. The results show the following:

1. At all locations along the inclusion, the tensile stress is a linear function of the stress ratio, R (for R≤8, corresponding to a mobilized friction angle, $\phi_{mob}=51^0$).
2. The maximum tensile stress occurs at the center of the inclusion. At a given stress ratio, R, there is a monotonic 'pick-up' in the tensile stress with distance from the tip of the inclusion.
3. There is minimal development of tensile stresses in the reinforcement for stress ratios, R≤2.

4. INTERPRETATION OF APSR DATA

In parallel with the design and construction of the APSR cell, analytical models have been developed to predict and interpret the load distribution within the reinforcement based on known (specified) properties of the soil and reinforcing materials. Initially, the analyses have assumed a) linear, isotropic and elastic properties for the soil matrix and reinforcement, and b) the planar inclusion is oriented parallel to the minor external principal stress in the soil (i.e., Fig. 4). Even for this simplified problem, complete analytical solutions are difficult to achieve.

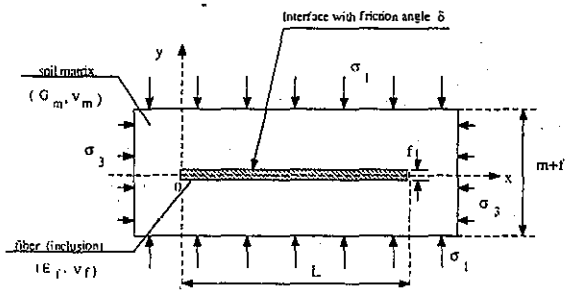

Fig. 4 Geometry of the reinforced soil element

Although comprehensive numerical analyses are possible using finite element methods, it is difficult to interpret how the various geometric and material properties affect the predictions of load transfer. Abramento and Whittle (1992) have presented an approximate analytical method which expresses the reinforcement stresses as closed form functions of the elastic properties of the constituent materials (i.e., soil matrix and reinforcement), inclusion geometry and interface friction. The formulation adapts the techniques of shear-lag analysis (Cox, 1952; Kuhn, 1956; Budiansky et al., 1986) which are widely used in the mechanics of fibre reinforced composites. The analytical solutions are in excellent agreement with numerical solutions obtained by finite element methods.

The shear lag analysis approximates the deformation field within the soil matrix such that the tensile stress in the planar inclusion, σ^f_{xx}, can be solved directly from equilibrium considerations. In the analysis presented by Abramento and Whittle (1992), the tensile stress in the inclusion can be written as a linear function of the external principal stresses, σ_1 and σ_3 (cf. Fig. 3):

$$\sigma^f_{xx} = \frac{K_2\sigma}{K_1}\left[1 - \frac{\cosh\sqrt{K_1}\left(\frac{L}{2} - x\right)}{\cosh\sqrt{K_1}\frac{L}{2}}\right] \qquad (1)$$

where,

$$K_2\sigma = K_2^1\sigma_1 + K_2^3\sigma_3 \qquad (2)$$

and the coefficients K_1, K_2 can be written in terms of the elastic properties of the soil and reinforcement material, and the geometry (Fig. 4):

$$K_1 = \frac{6}{mf}\frac{\left[(1-\nu_m)a + 2\frac{G_m}{E_f}(1+\nu_f)(1-\nu_f)\right]}{\left[1+\frac{1}{4}\nu_m - \frac{3}{2}\frac{G_m}{E_f}(1+\nu_f)\nu_f\right]}$$

$$K_2^1 = \frac{6}{mf}\frac{\left[\nu_m - 2\frac{G_m}{E_f}(1+\nu_f)\nu_f\right]}{\left[1+\frac{1}{4}\nu_m - \frac{3}{2}\frac{G_m}{E_f}(1+\nu_f)\nu_f\right]}$$

$$K_2^3 = -\frac{6}{mf}\frac{(1-\nu_m)(1+a)}{\left[1+\frac{1}{4}\nu_m - \frac{3}{2}\frac{G_m}{E_f}(1+\nu_f)\nu_f\right]}$$

where G_m, E_f are the elastic shear modulus of the soil matrix and Young's modulus of the reinforcement; ν_m, ν_f are the respective Poisson ratios; the dimensions f, m are shown in figure 4; and a=f/m.

Thus the maximum load carried by the rcinforcement in a very long inclusion is given by:

$$\sigma^f_\infty = \left(\sigma^f_{xx}\right)_{L=\infty} = \frac{K_2\sigma}{K_1} \qquad (3)$$

For inclusions of finite length (L/2≤0.45m, in the APSR cell), the maximum tensile stress at the center of the inclusion, $\sigma^f_{max}=\sigma^f_{xx}(L/2)$, is controlled by the shear lag parameter, K_1. Figure 5 summarizes the maximum load transfer ratio', $\sigma^f_{max}/\sigma^f_\infty$ as a function of the inclusion length, L, and the stiffness ratio, E_f/G_m, for an inclusion with thickness, f=1 mm, and matrix spacing, m=0.5m. The results show that the 'pick-up length' necessary to achieve maximum load transfer (i.e., σ^f_{max}->σ^f_∞) increases significantly with the stiffness ratio. For a realtively inextensible reinforcement such as steel ($E_f/G_m\approx10^4$, Fig. 3), the

pick-up length, L/2≈1.5m, which is significantly longer than the dimensions available in the APSR cell. Thus, predictions of stresses in a prototype (field) situation must be estimated by extrapolating the APSR measurements from tests performed on inclusions of different lengths. In contrast, full pick-up is expected for more extensible reinforcing materials ($E_f/G_m=10^2$, Fig. 5) including various types of geosynthetics. Abramento and Whittle (1992) also show that, for practical values of interface friction, $\delta=10^0$-30^0, interface slippage has minimal effect on the maximum load transfer.

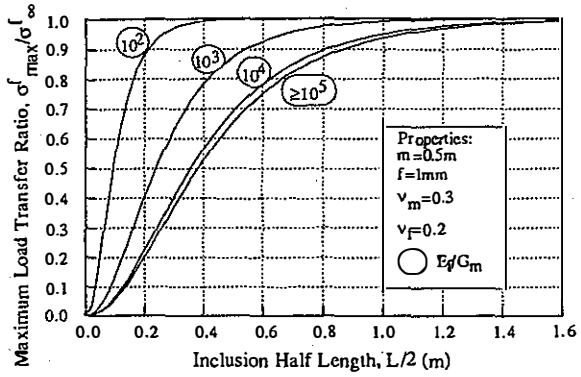

Fig. 5 Effect of inclusion length and stiffness on maximum load transfer ratio

Figure 6 summarizes the maximum tensile stresses (for long inclusions), σ^f_∞/σ_3, as a function of the external stress ratio, for ranges of material properties E_f/G_m, ν_m, and the reinforcement volume ratio, f/m. The results show the following:

1. There is no load transfer when the external stress ratio, $\sigma_1/\sigma_3=1/K_0=(1-\nu_m)/\nu_m$.
2. The reinforcement stress increases significantly with the stiffness ratio, E_f/G_m. However, close spacing of reinforcing layers (high f/m; Fig. 6b) reduces the benefits of high stiffness ratios. For example, calculations for a volume ratio, a=0.02 (Fig. 6b), show similar load transfer behavior for reinforcements with $E_f/G_m=10^3$, 10^4.
3. As ν_m increases from 0.3 to 0.5, the reinforcement stress increases by a factor of 2 to 3 (Fig. 6a). This behavior confirms the underlying mechanism whereby tensile stresses in the reinforcement counteract lateral straining of the soil matrix.

The results in figure 6 provide a basis for quantifying the reinforcing effect of the inclusion on the soil matrix. However, there are two important limitations on the interpretation of these results:

1. For drained shearing of cohesionless soils, the shear strength is most commonly described by a Mohr-Coulomb failure criterion with friction angle, ϕ. Ladd et al (1977) report $35^0 \leq \phi \leq 57^0$ (i.e., $3.7 \leq \sigma_1/\sigma_3 \leq 11.7$) for typical sands sheared in plane strain compression. Thus, local failure will initiate in the matrix (at locations close to the tip of the inclusion) when the frictional strength of the soil is mobilizerd and will affect the load transfer to the reinforcing inclusion.
2. The linear, isotropic model of soil behavior does not describe accurately the volumetric response of cohesionless soils in drained shearing. Extensive observations show that sands dilate when the mobilized friction exceeds a threshold value, $\phi_{cv}=35^0$ to 45^0 (σ_1/σ_3 = 3.7 to 5.8) (Bolton, 1986; Larson, 1992). The practical implication of this behavior is that the proposed analysis will tend to underestimate both the lateral strains occuring in the soil matrix and tensile stresses in the reinforcement when the soil dilates at high external stress ratios (i.e., R≥6-8).

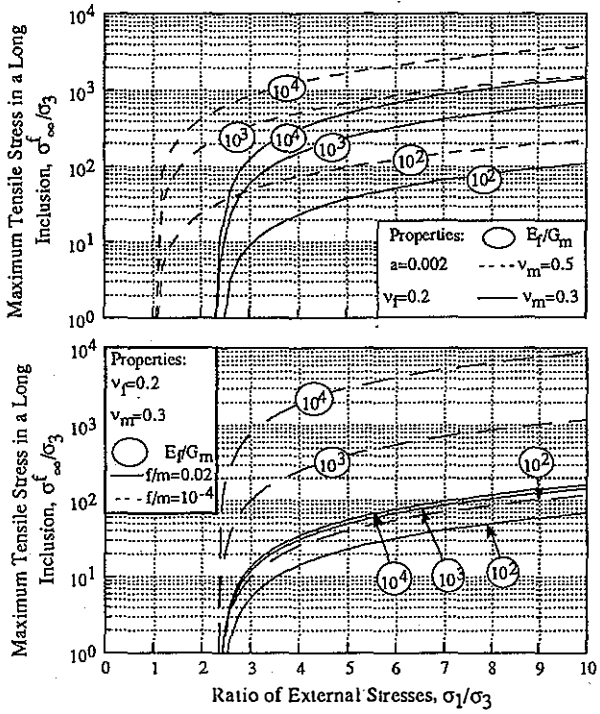

Fig. 6 Load transfer for long inclusions

5. EVALUATION OF APSR MEASUREMENTS

The shear lag analyses provide a simple framework for evaluating measurements in the APSR cell at working stress levels. Figure 7 compares predictions with APSR cell measurements of tensile stresses in a steel sheet inclusion. The analytical predictions use elastic material properties determined from plane strain shear tests (on the unreinforced sand in the APSR cell), and in-isolation, uniaxial tension tests on the steel sheet inclusion. The predictions are in good agreement with both the distribution and magnitudes of tensile stresses measured by the APSR cell at stress ratios, R=3 and 6. These results: a) confirm the capabilities of the APSR cell for measuring reliably the tensile stresses which develop in an elastic inclusion due to shearing of the surrounding soil; and b) demonstrate that the proposed shear lag analysis

provides a realistic basis for interpreting load transfer in reinforced soils.

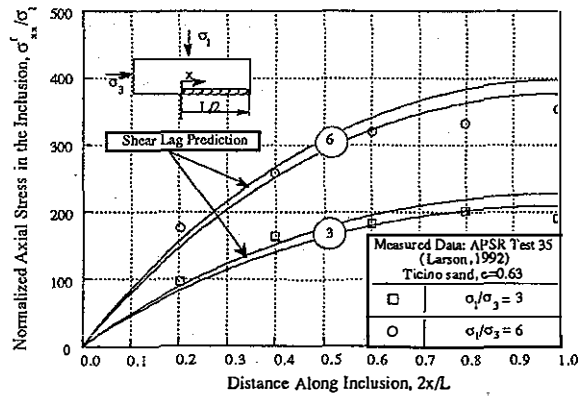

Fig. 7 Evaluation of load transfer predictions

6. CONCLUSIONS

This paper summarizes the design of a new laboratory device, referred to as the APSR cell, which is capable of measuring the maximum tensile stress that develops in a planar inclusion due to shearing of the surrounding soil. Measurements of load transfer for an elastic steel sheet inclusion demonstrate the capabilities of the new device. The APSR cell represents a controlled laboratory experiment that will enable direct comparisons of load-transfer charactersitics for different types of reinforcing material.

An approximate shear lag analysis has also been developed in order to predict and interpret measurements in the APSR cell. The analysis describes the tensile stresses in the inclusion assuming that the soil matrix and reinforcement act as linear, elastic materials linked through a frictional interface. The solutions show clearly how the material properties and geometry affect the load transfer for a planar reinforcement. Direct comparisons show that the shear lag analysis can predict accurately the tensile stresses measured in the APSR cell for an elastic steel sheet inclusion.

ACKNOWLEDGEMENT

This work was supported by the US Army Research Office through the MIT Program for Advanced Construction Technology.

REFERENCES

Abramento, M. and Whittle, A.J. 1992. Shear lag analysis of a planar soil reinforcement in plane strain compression. *submitted ASCE Journal of Engineering Mechanics.*

Arthur, J.R.F. 1977. Industrial radiography in soil mechanics. British Journal of Non-Destructive Testing. 29(1): 9-13.

Arthur, J.R.F., and Menzies, B.K. 1972. Inherent anisotropy in a sand. Géotechnique 22(1): 115-128.

Baldi, G. et al. 1985. Laboratory validation of in-situ tests. Proc. 11th International Conference on Soil Mechanics and Foundation Engineering, San Fransisco, AGI Jubilee Volume: 251-270.

Bolton, M.D. 1986. The strength and dilatancy of sands. Géotechnique, 36(1):65-79.

Budiansky, B., Hutchinson, J.W., and Evans, A.G. 1986. Matrix fracture in fiber-reinforced ceramics. Journal of Mechanics and Physics of Solids 34(2): 167-189.

Cox, H.A. 1952. The elasticity and strength of paper and other fibrous materials. British Journal of Applied Physics, 3:72-79.

Jewell, R.A. 1990. Strength and deformation in reinforced soil design. Proc. International Conference on Geotextiles, Geomembranes & Related Products, The Hague, Netherlands, 79p.

Jewell, R.A. and Wroth, C.P. 1987. Direct shear tests on reinforced sand. Géotechnique, 37(1): 53-68.

Kuhn, P. 1956. Stresses in aircraft and shell structures. McGraw-Hill.

Ladd, C.C., Foott, R., Ishihara, K., Schlosser, F. and Poulos, H.G. 1977. Stress-deformation and strength characteristics. Proc. 9th International Conference on Soil Mechanics and Foundation Engineering, Tokyo, 2:421-494.

Larson, D.G. 1992. PhD Thesis in progress, MIT, Cambridge, MA.

Marachi, N.D., Duncan, J.M., Chan, C.K., and Seed, H.B. 1981. Plane-Strain Testing of Sand. Laboratory Shear Strength of Soil, American Society for Testing and Materials ASTM STP 740: 294-302.

McGown, A., Andrawes, K.Z., and Al-Hasani, M.M. 1978. Effect of inclusion properties on the behaviour of sand. Géotechnique, 28(3): 327-346.

McGown, A., Andrawes, K.Z. and Yeo, K.C. 1985. The load-strain-time behaviour of Tensar geogrids. Proc. ICE Conference on Polymer Grid Reinforcement, London: 11-17.

Palmeira, E.M., and Milligan, G.W.E. 1989. Large scale direct shear tests of reinforced soils. Soils and Foundations 9(1): 18-30.

Schlosser, F. and Long, N.T. 1972. Comportement de la terre armée dans les ouvrages de soutènement. Proc. 5th European Conference on Soil Mechanics and Foundation Engineering, Madrid. 1: 299-306.

Shewbridge, S.E., and Sitar, N. 1989. Deformation characteristsics of reinforced sand in direct shear. ASCE Journal of Geotechnical Engineering 115(8): 1134-1147.

Whittle, A.J., Larson, D.G., Abramento, M. and Germaine, J.T. 1991. Geosynthetic reinforcement of soil masses. Annual Technical Report submitted to US Army Research Office.

Wilding, M.A. and Ward, I.M. 1978. Tensile creep and recovery in ultra-high modulus linear polyethylenes. Polymer 19(8):969-976.